JEM Journal of Experimental Medicine

ARTICLE

Loss of human ICOSL results in combined immunodeficiency

Lucie Roussel[1], Marija Landekic[1], Makan Golizeh[1], Christina Gavino[1], Ming-Chao Zhong[2], Jun Chen[2], Denis Faubert[3], Alexis Blanchet-Cohen[4], Luc Dansereau[5], Marc-Antoine Parent[6], Sonia Marin[7], Julia Luo[1], Catherine Le[1], Brinley R. Ford[1], Mélanie Langelier[1], Irah L. King[8,11], Maziar Divangahi[8,11,12], William D. Foulkes[9,10], André Veillette[2,11,13], and Donald C. Vinh[1,2,10,11]

Primary immunodeficiencies represent naturally occurring experimental models to decipher human immunobiology. We report a patient with combined immunodeficiency, marked by recurrent respiratory tract and DNA-based viral infections, hypogammaglobulinemia, and panlymphopenia. He also developed moderate neutropenia but without prototypical pyogenic infections. Using whole-exome sequencing, we identified a homozygous mutation in the inducible T cell costimulator ligand gene (*ICOSLG*; c.657C>G; p.N219K). Whereas WT ICOSL is expressed at the cell surface, the ICOSL^{N219K} mutation abrogates surface localization: mutant protein is retained in the endoplasmic reticulum/Golgi apparatus, which is predicted to result from deleterious conformational and biochemical changes. ICOSL^{N219K} diminished B cell costimulation of T cells, providing a compelling basis for the observed defect in antibody and memory B cell generation. Interestingly, ICOSL^{N219K} also impaired migration of lymphocytes and neutrophils across endothelial cells, which normally express ICOSL. These defects likely contributed to the altered adaptive immunity and neutropenia observed in the patient, respectively. Our study identifies human *ICOSLG* deficiency as a novel cause of a combined immunodeficiency.

Introduction

Primary immunodeficiencies are inborn errors of immunity, marked by increased susceptibility to infections, auto-inflammation, auto-immunity, atopy, and/or increased risk for lymphoproliferative or malignant disorders (Picard et al., 2018). The microbial spectrum of pathogens can be broad or restricted, causing infections that may be fulminant and life-threatening or chronic and recalcitrant to standard therapy (Casanova and Abel, 2018). Elucidating the molecular basis of these rare disorders provides unique insight into human immunobiology.

Combined immunodeficiencies (CIDs) comprise a heterogeneous group of disorders due to quantitative and/or functional T and B cell defects. In its most severe form, severe combined immunodeficiency (SCID), typically null mutations arrest lymphocyte development and result in the absence of autologous T cells, which leads to life-threatening complications in early infancy. On the other hand, those that permit survival beyond early childhood (the so-called "leaky" or "partial" SCID, or simply CID) are marked by the production of T and B cells, albeit in subnormal quantity and/or function (Notarangelo, 2014). In some cases, CID may be due to "leaky" genetic phenomena, such as hypomorphic mutations or mosaicism, permitting the less severe clinical evolution of disease; other cases represent novel genetic etiologies. In recent years, a subset of CIDs, distinctly characterized by the combined defects of both lymphoid and myeloid lineages, without global marrow aplasia, has been reported (Dotta and Badolato, 2014; Lagresle-Peyrou et al., 2016; Afzali et al., 2017).

Inducible T cell costimulator (ICOS) is expressed on the surface of activated T cells (Nurieva et al., 2003). Through cognate interaction with inducible T cell costimulator ligand (ICOSL) expressed on the surface of a variety of cells, particularly APCs,

[1]Infectious Disease Susceptibility Program, McGill University Health Centre and Research Institute–McGill University Health Centre, Montréal, Québec, Canada; [2]Laboratory of Molecular Oncology, Institut de recherches cliniques de Montréal, Montréal, Québec, Canada; [3]Proteomics Discovery Platform, Institut de recherches cliniques de Montréal, Montréal, Québec, Canada; [4]Bioinformatics, Institut de recherches cliniques de Montréal, Montréal, Québec, Canada; [5]Department of Internal Medicine, Hôpital de l'Archipel, Centre intégré de santé et de services sociaux des Îles, Les Îles-de-la-Madeleine, Québec, Canada; [6]Department of Family Medicine, Centre intégé de santé et de services sociaux des Îles, Les Îles-de-la-Madeleine, Québec, Canada; [7]Hôpital de l'Archipel, Centre intégré de santé et de services sociaux des Îles, Les Îles-de-la-Madeleine, Québec, Canada; [8]Meakins-Christie Laboratories, Research Institute–McGill University Health Centre, Montréal, Québec, Canada; [9]Department of Medical Genetics, Research Institute–McGill University Health Centre, Montréal, Québec, Canada; [10]Department of Human Genetics, McGill University, Montréal, Québec, Canada; [11]Department of Medicine, McGill University, Montréal, Québec, Canada; [12]Department of Microbiology and Immunology, McGill University, Montréal, Québec, Canada; [13]Department of Medicine, University of Montréal, Montréal, Québec, Canada.

Correspondence to Donald C. Vinh: donald.vinh@mcgill.ca; A. Blanchet-Cohen's current address is Department of Human Genetics, Segal Cancer Centre and Lady Davis Institute, Jewish General Hospital, McGill University, Montréal, Québec.

adaptive immunity is generated (Nurieva et al., 2003). Humans with bi-allelic loss-of-function mutations in *ICOS* were initially identified as having hypogammaglobulinemia with recurrent bacterial infections (diagnosed as "common variable immunodeficiency"; Grimbacher et al., 2003; Salzer et al., 2004; Warnatz et al., 2006). Subsequent reports demonstrate that such patients are also at risk for infections typical of T cell dysfunction (e.g., with human papillomavirus [HPV], *Cryptococcus*), categorizing ICOS deficiency as a CID (Robertson et al., 2015; Schepp et al., 2017). Moreover, NF-κB–inducing kinase (NIK) deficiency (due to bi-allelic mutations in *MAP3K14*) is a recently defined cause of human CID; one consequence of absent NIK function is loss of induced *ICSOLG* expression (Willmann et al., 2014). To date, however, no monogenic defects in *ICOSLG* have been reported. In this study, we describe a patient with CID associated with autosomal recessive *ICOSLG* deficiency.

Results

Clinical and immunological phenotype of patient 1 (P1)

The proband, patient 1 (P1), is a male born to French-Canadian parents in Les Îles de la Madeleine, a geographically isolated island of the province of Quebec, Canada. Although multiple ancestral generations have lived on that island, there was no known direct consanguinity between his parents. Since childhood, he experienced several episodes of otitis media per year, although none were refractory to therapy or severe enough to require intravenous antibiotics, hospitalization, or tympanostomy tubes. He also had recurrent sinusitis approximately once per year of similar severity, as well as several episodes of bronchitis. At age 21, he had one episode of pneumonia requiring hospitalization.

In early childhood, he recalled having warts on the arms and neck that required local destructive therapy without recurrence. At age 16, he developed genital warts. Despite various therapies, the condylomata recurred in the same penile region and spread over the years to involve the scrotum, perineum, perianal, and inguinal regions; by age 33, he had urethral involvement, which was eventually controlled with regular topical self-application of 5-fluorouracil. Since adolescence, he has also had recurrent, microbiologically confirmed oro-labial HSV infections. Since age 29, he has developed recurrent febrile episodes of oral apthous-like ulcers, for which no microbiologic cause was identified. He has also repeatedly had angular cheilitis.

Limited immunological investigations at a regional health center at age 29 revealed hypogammaglobulinemia and panlymphopenia with normal proportions. He was also found to have moderate neutropenia; in review of his previous blood work, the neutrophil count had steadily declined over the preceding years (Tables 1, 2, and 3). Despite this, he had no history of serious pyogenic infections typical of neutropenia (e.g., periodontal disease, skin and soft tissue infection). He failed to seroconvert to tetanus, diphtheria, and *Haemophilus influenzae* type B; responses to polysaccharide vaccination were not tested. Antibodies to neutrophils were not detected. He was started on intravenous immunoglobulin replacement, which significantly improved the frequency of respiratory tract infections. Persistence of the neutropenia prompted a bone marrow examination, which revealed normocellularity, complete granulocyte maturation with no myelokathexis or myelodysplasia, with ∼5% of cells being small lymphocytes, predominantly of T cell origin. Sequencing of *CXCR4* identified no mutation. The neutrophil count quantitatively normalized on G-CSF therapy and returned to basal levels when it was stopped.

Table 1. **Immunophenotyping data of P1 at ages 29–35**

Parameter	Age (yr)		
	29	30–32	33–35
ANC	3,100	924–1,862 (↓)	341–1,000 (↓)
AMC	412	60–566	13–1179
ALC	700 (↓)	588–849 (↓)	210–720 (↓)
CD3	525 (↓)	423–645 (↓)	259–469 (↓)
CD4	420	306–501 (↓)	190–301 (↓)
CD8	98 (↓)	112–136 (↓)	68–154 (↓)
CD19	98 (↓)	88–114 (↓)	68–144 (↓)
NK	49 (↓)	47–48 (↓)	43–90 (↓)
IgG	2.8 (↓)	6.1–15.15[a]	10.9–17.6
IgA	0.19 (↓)	0.15–0.2 (↓)	0.16–0.3 (↓)
IgM	0.85	0.52–0.77	0.66–0.76
IgE	7	NP	NP

Because the measurements were performed in various clinical laboratories, ↓ indicates that at least one of the measurements during this time was lower than the reference range of the corresponding laboratory. ↑ indicates that at least one measurement was higher than the controls. ANC, absolute neutrophil count; AMC, absolute monocyte count (as evaluated by automated or manual differential count); ALC, absolute lymphocyte count; NP, not performed.
[a]After commencing intravenous immunoglobulin therapy.

The patient was referred for further investigations at age 35, which confirmed the T lymphopenia, with severely reduced naive $CD4^+$ T cells, B lymphopenia with severely reduced memory B cells, slightly decreased NK cells, and moderate neutropenia. In-depth immunophenotyping at age 38 demonstrated the following (Tables 1, 2, and 3). Circulating absolute neutrophil count was mildly decreased, whereas absolute $CD14^+$ monocyte count was similar to controls. The proportion of T regulatory (T reg) cells ($CD4^+$ $FoxP3^+$) and total conventional dendritic cells (DCs; $Lineage^-$ $CD11c^+$), as well as the major subsets ($CD1c^+$, $CD141^+$) were similar to controls. Circulating total T follicular helper (Tfh) precursor cells ($CD4^+$ $CXCR5^+$) were similar to healthy controls (HCs); however, the Tfh subtypes were vastly different, with P1 demonstrating an elevated proportion in the Tfh partial effector phenotype ($CD45RA^-$ $CD4^+$ $CXCR5^+$ $PD\text{-}1^{hi}$ $CCR7^{lo}$) with decreased levels of Tfh resting phenotype ($CD45RA^-$ $CD4^+$ $CXCR5^+$ $PD\text{-}1^{lo}$ $CCR7^{hi}$; Fig. S1), as defined by He et al. (2013). Circulating B cells were nearly all naive, with near absence of switched memory B cells. Thus, P1 had clinical and immunological features of a combined deficiency of adaptive immunity with slowly progressive neutropenia.

Homozygous p.N219K variant in *ICOSLG*

Whole-exome sequencing (WES) was performed on P1. Given the ancestral geographical isolation, an autosomal recessive pat-

Table 2. **Immunophenotyping data of P1 at age 35**

Parameter	Result
ANC	400 (↓)
AMC	600
ALC	600
CD3	420 (70%; ↓)
CD4	288 (48%; ↓)
CD8	104 (17.4%; ↓)
CD4/CD45RA	54 (9%; ↓)
CD4/CD45RO	16 (2.6%; ↓)
CD19	7 (1.2%; ↓)
CD19/CD27	6 (1%; ↓)
$CD3^+/CD56^+$	25 (4.1%)
$CD3^-/CD56^+$	109.2 (18.2%)

Because the measurements were performed in various clinical laboratories, ↓ indicates that at least one of the measurements during this time was lower than the reference range of the corresponding laboratory. ↑ indicates that at least one measurement was higher than the controls. ANC, absolute neutrophil count; AMC, absolute monocyte count (as evaluated by automated or manual differential count); ALC, absolute lymphocyte count.

Table 3. **In-depth immunophenotyping data of P1 at age 38**

Parameter	Result	Reference range[a]
ANC	1,140 (↓)	1,500–7,700/ml
$CD14^+$ monocytes	330	165–780/ml
ALC	670	1,000–4,800/µl
$CD3^+$ T cells	387 (↓); 62%	661–2,224/ml
$CD4^+$ T cells	281 (↓); 45%	356–1,573/ml
$CD8^+$ T cells	92 (↓); 15%	113–804/ml
Circulating Tfh cells[b]	12%	13.4–24.9%
Partial effector Tfh cells[c]	22.9% (↑)	9.26–11.1%
Resting memory Tfh cells[d]	30.6% (↓)	60.5–69%
T reg cells[e]	7.74%	6.85–8.65%
$CD19^+$ B cells	159; 26%	143–396/ml
Naive B[f]	97.8% (↑)	14–58%
Switched memory B[g]	0.16% (↓)	23–60%
$CD3^-/16^+$ or 56^+	67 (↓); 11%	82–594/ml
$CD11c^+$ conventional DC[h]	3.29%	1.75–4.59%
$CD1c^{+i}$	3.38%	0.95–3.18%
$CD141^{+j}$	3.01%	1.33–3.09%

Because the measurements were performed in various clinical laboratories, ↓ indicates that at least one of the measurements during this time was lower than the reference range of the corresponding laboratory. ↑ indicates that at least one measurement was higher than the controls. ANC, absolute neutrophil count; ALC, absolute lymphocyte count.
[a]Reference ranges from HCs.
[b]$CD45RA^-$ $CD4^+$ $CXCR5^+$.
[c]$CD45RA^-$ $CD4^+$ $CXCR5^+$ PD-1^{hi} $CCR7^{lo}$.
[d]$CD45RA^-$ $CD4^+$ $CXCR5^+$ PD-1^{lo} $CCR7^{hi}$.
[e]$CD4^+$ $Foxp3^+$.
[f]$CD45^+$ $CD19^+$ $CD27^-$ IgD^+.
[g]$CD45^+$ $CD19^+$ $CD27^+$ IgD^-.
[h]$Lin1^-$ HLA-DR^+ $CD11c^+$.
[i]$Lin1^-$ HLA-DR^+ $CD11c^+$ $CD1c^+$.
[j]$Lin1^-$ HLA-DR^+ $CD11c^+$ $CD141^+$.

tern of inheritance was suspected. Mutations in known primary immunodeficiency genes were not identified (see Table S1 for a comprehensive list of identified genetic variants with respective scores for deleteriousness). However, a novel homozygous variant in exon 4 of *ICOSLG* (c.657C>G), predicted to change the asparagine at amino acid 219 to lysine (p.N219K), was detected (Fig. 1 A). The N219 residue is highly conserved from humans to lamprey (UCSC Genome Browser). This residue is located in the extracellular portion of the molecule, in the immunoglobulin-like C2-type domain (Fig. 1 B). This variant is not in dbSNP build 142 (however, it was subsequently reported in build 147 at a frequency of 1/20,934, i.e., 0.005%); it is not reported in Broad Exome Aggregation Consortium (ExAC browser) database or in 1000 Genomes, and is thus exceedingly rare. The p.N219K variant is predicted in silico (i.e., PolyPhen2, SIFT, MutationTaster) to be maximally deleterious. Sanger sequencing confirmed that P1 was homozygous for this variant, whereas his parents were heterozygous and his healthy brother was homozygous for the WT allele; thus, the p.N219K variant segregates with the phenotype in the patient's pedigree.

Loss of cell-surface expression of ICOSL p.N219K

Given the geographic distance and pan-leukopenia of P1, primary cells were limited. We thus first characterized the impact of the p.N219K variant on ICOSL production in EBV-transformed B-lymphoblastoid cell lines (LCLs) from P1 and controls. RT-PCR demonstrated comparable *ICOSLG* mRNA levels, indicating that the variant did not result in significant mRNA decay; however, total ICOSL protein levels from LCL whole-cell lysates from P1 were reduced relative to controls (Fig. 2 A). Flow cytometric analysis, using two different antibodies recognizing distinct epitopes of ICOSL, showed that its cell-surface expression was absent in P1; however, this was not due to variant-associated changes in epitope recognition, as intracellular staining detected ICOSL in P1's LCL (Fig. 2 B).

Confocal microscopy likewise demonstrated decreased cell-surface expression, with accumulation of ICOSL in the juxtanuclear position of P1's LCL, predominantly in the Golgi complex by organelle staining (Fig. 2 C). We observed a similar phenomenon following transient transfection of HEK293T cells, which lack endogenous ICOSL, with either WT or p.N219K ICOSL protein (data not shown). Collectively, these data indicate that the mutant ICOSL is produced but fails to be properly expressed at the cell surface due to intracellular retention. Thus, the p.N219K allele is deleterious at the molecular level.

Molecular characterization of the p.N219K mutation

To better understand the mechanism leading to absent cell-surface expression of ICOSL, we first analyzed in silico the impact of the p.N219K mutation on posttranslational modification

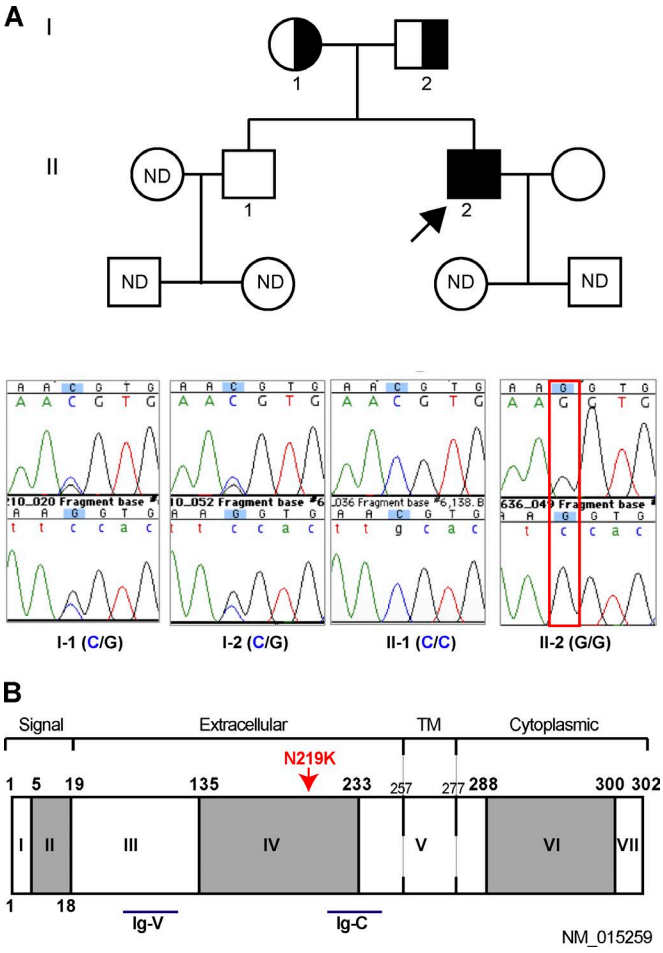

Figure 1. **Autosomal recessive ICOSLG deficiency. (A)** Pedigree analysis, showing familial segregation of the c.657C>G (p.N219K) mutant *ICOSLG* allele. Generations are designated by Roman numerals. Proband (P1) is indicated by the arrow. **(B)** Schematic representation of the ICOSL protein. The exons are numbered with Roman numerals and represented in alternating gray and white boxes. TM, transmembrane. The different domains, as well as the Ig-V and Ig-C loops, are depicted, with their corresponding amino acid boundaries numbered accordingly. The p.N219K mutation is identified by the arrow.

(PTM). ICOSL is predicted to have four N-glycosylation sites (NetNGlyc 1.0), at N70, N137, N186, and N225. Given that N219 is not among these, loss of N-glycosylation at this residue is not anticipated with the mutation. The substitution to lysine may result in a gain of PTM. Although such changes typically regulate the activity of proteins during immune pathway signaling (Mowen and David, 2014), they may potentially affect protein trafficking. The 219K is not predicted to result in gain of methylation (MethK; GPS-MSP), acetylation (GPS-PAIL), ubiquitination (iUbiq-Lys), or SUMOylation (JASSA). These models predict that alteration of these PTMs in ICOSL is not the basis for the deleterious effect of the N219K mutation. Supporting this, Western blot analysis of whole-cell lysates from LCL revealed no differences in the profile of ICOSL migration between WT and mutant (Fig. 2 A).

We further sought to analyze the effect of the missense mutation on protein structure. In the absence of an experimentally determined three-dimensional (3D) structure of ICOSL, we used homology modeling (Swiss-Model ExPASy) using mouse CD276 antigen (Protein Data Bank entry 40ik) as the most closely related, available template (Global Model Quality Estimation [GMQE] 0.59–0.68) to investigate how the N219K substitution in the extracellular region abrogates cell-surface expression (Fig. S2 A). Secondary structure prediction modeling (MeDor 1.4) suggests that N219K modifies the coil/strand hybrid structure of the [215–222] region in the WT protein, to a pure coil in the mutant (Fig. 3, A and B); the predicted conformational change at the site of mutation is shown (Fig. 3, C and D). Disordered domain analysis (DisEMBL 1.5) also predicts modified loop stability as a result of N219K mutation, with reduction in the length of the loops: from [206–216] and [226–253] in the WT ICOSL to [206–215] and [227–253] in the mutant. This modification is predicted to impart less molecular rigidity (Fig. S2, B–D).

Lastly, while the transmembrane topology (by Phobius) of ICOSL is predicted to be unaffected by N219K, the biochemical properties of the protein are altered, with increased hydrophilicity by 8.5% (GRAVY calculator) and basicity by 2.3% (ExPASy) in the mutant protein. Attempts to increase cell-surface expression of intracellular-retained protein, by incubating P1's cells at various temperatures (e.g., 37°C, 27°C, and 15°C), stimulating cells with various cytokines (e.g., GM-CSF; TNFα), or treating cells with inhibitors of protein degradation (i.e., inhibitors of proteasome [bortezomib; MG132], lysosome [bafilomycin; chloroquine], or aggresome [tubacin]), were not successful (data not shown). Altogether, the changes in secondary structure, conformation, disorder, and biochemistry caused by p.N219K are anticipated to hinder the translocation of the mutant ICOSL across the plasma membrane.

Mutant ICOSL is defective in T cell costimulation

ICOSL is normally expressed on the surface of APCs, providing costimulation through ICOS on the surface of activated T cells in the germinal centers (GCs) of lymph nodes, permitting effective development of antibody-mediated immunity. Given the absent cell-surface expression of p.N219K ICOSL on P1's LCL, we sought to determine the functional consequences of the mutation on T cell costimulation. Because ICOS–ICOSL interaction has been previously shown to modulate cytokine secretion through its effects on recently activated mature T cells (Hutloff et al., 1999), we cocultured Jurkat cells, at resting state or activated by TNFα to induce ICOS expression (Fig. 4 A), with LCL from HCs) or P1, and measured induced gene responses of cytokines by quantitative PCR (qPCR).

P1's LCLs were significantly impaired in their ability to induce the genes for cytokines critical for T cell–dependent high-affinity antibody responses (IL-2, IL-4, and IL-21; Fig. 4 B). This defect was also seen when TNFα-activated primary T cells from HC were cocultured with P1's LCL, but not with HC LCL (Fig. 4 C). Reduction of these cytokine responses following ICOSL blockade on HC LCLs, and complementation experiments (in which expression of WT *ICOSLG* in P1's LCLs rescues their capacity to stimulate Jurkat cells; Fig. 4 D), confirm that this costimulatory effect was specifically due to ICOSL. Hence, expression of $ICOSL^{N219K}$ in B cells results in compromised ability to provide T cell costimulation.

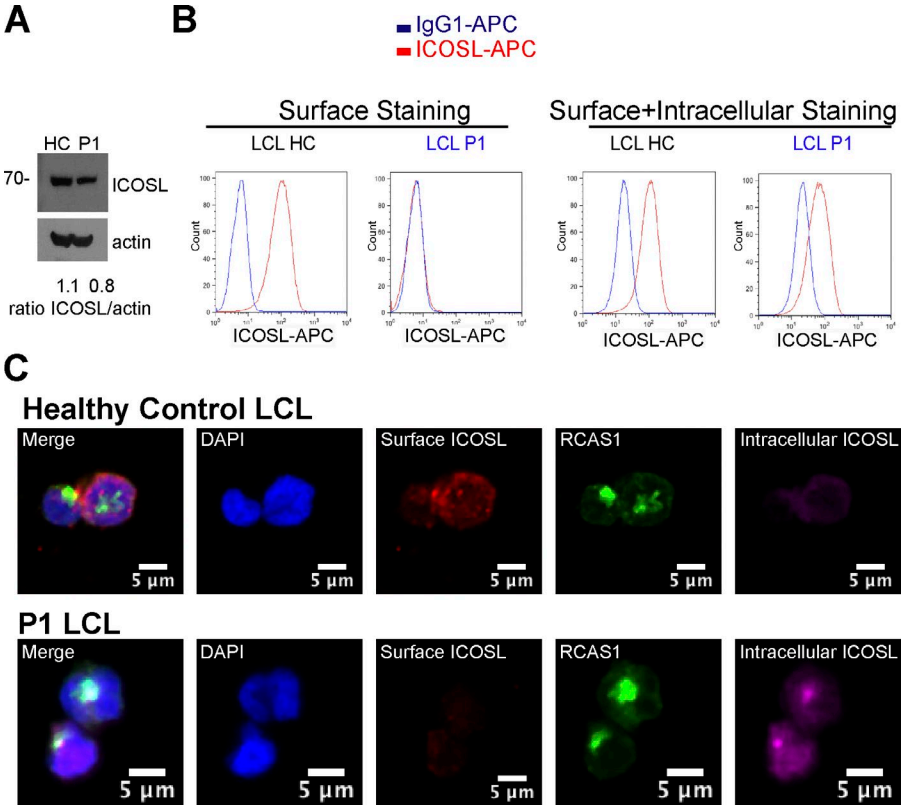

Figure 2. **Molecular impact of the p.N219K mutation in ICOSL. (A)** Western blot analysis of whole-cell lysates from subject-derived LCLs; β-actin served as a loading control. **(B)** ICOSL expression determined by flow cytometry on CD19⁺ gated, live LCL, either at the cell surface alone or combined cell-surface and intracellular staining. MIH12 monoclonal antibody shown. **(C)** Confocal microscopy of LCL from HC or P1. ICOSL expression was probed for cell-surface expression (alone) or combined cell-surface and intracellular staining using two secondary antibodies conjugated to different fluorophores. Markers for nucleus (DAPI), Golgi (RCAS1), and overlaid images are shown. Data are representative of three independent experiments.

ICOSL^{N219K} expression in endothelial cells compromises T cell transendothelial migration

ICOSL is also expressed on endothelial cells (Khayyamian et al., 2002). Because primary endothelial cells from P1 were not available due to ethical constraints, we sought to assess the impact of ICOSL deficiency on lymphocyte trafficking, by testing the migration of TNFα-activated Jurkat cells (Fig. 5 A) across human microvascular endothelial cells (HMEC-1) that were silenced for endogenous *ICOSLG* and then transfected with either ICOSL WT or N219K. As seen with transfected HEK293T cells, HMEC-1 cells transfected with mutant ICOSL had significantly decreased expression of protein at the cell surface (Fig. S3, A and B). Transendothelial migration of Jurkat cells across p.N219K-transfected cells was significantly reduced relative to those transfected with ICOSL WT (Fig. 5 B). Thus, ICOSL deficiency impairs endothelial-guided migration of activated T cells.

Expression of mutant ICOSL in endothelial cells also interferes with neutrophil transmigration

Lastly, we sought to understand the basis for P1's neutropenia. We found that human neutrophils from healthy subjects do not express ICOS on the cell surface or intracellularly (data not shown), although they do produce ICOSL (Fig. 6 A). Due to

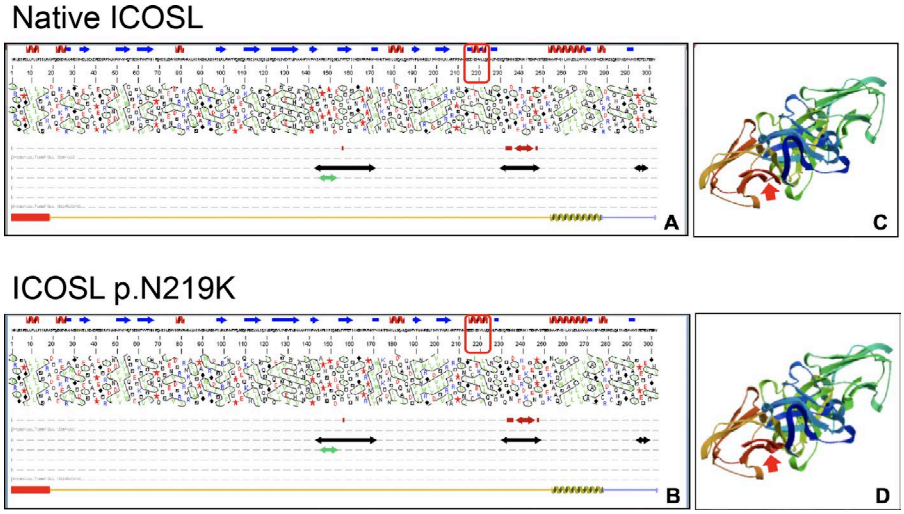

Figure 3. **Predicted structural conformation of native and mutant ICOSL. (A–D)** The N219K mutation is predicted to modify ICOSL conformation, from a mixed coil and strand of the [215–224] region to a full coil structure (A vs. B). This modification alters the secondary structure of the protein's extracellular region, potentially affecting its translocation to cell surface (C vs. D). Structural conformation prediction was performed by MeDor 1.4. Molecular 3D modeling was done by Swiss-Model/ExPASy using mouse CD276 antigen (Protein Data Bank entry 40ik) as the most closely related available template with a GMQE 0.59–0.68.

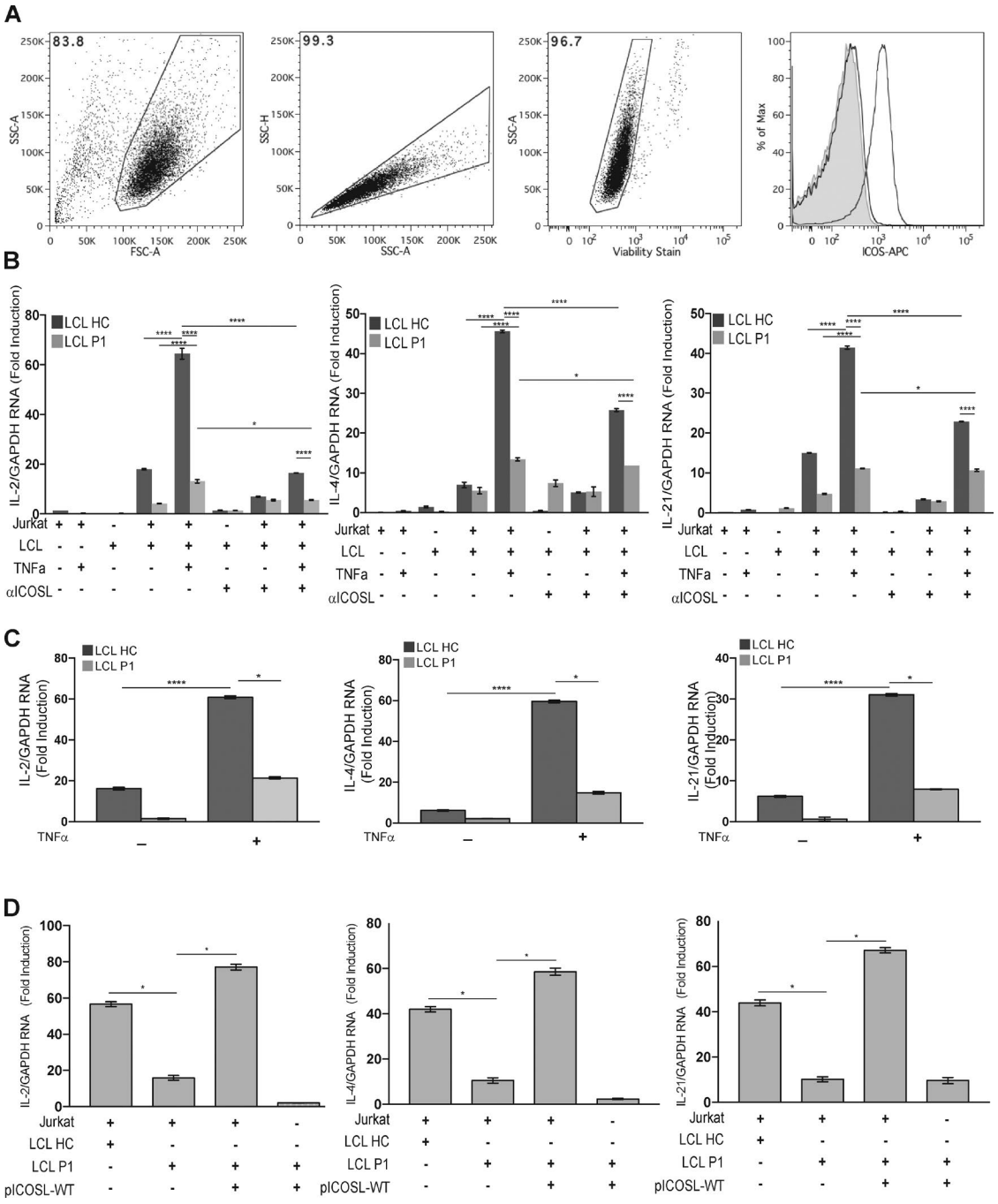

Figure 4. **Impaired ICOSL costimulation of T cells. (A)** Flow cytometry analysis of cell-surface expression of ICOS on Jurkat cells. Live-cell gating strategy shown. Unstimulated cells (filled line) and TNFα stimulation (dotted line) are shown relative to isotype control (shaded). **(B–D)** Expression of *IL2*, *IL4*, and *IL21*, as determined by qRT-PCR, following 6-h coculture of TNFα-activated Jurkat cells (B) or T cells from HCs (C), with LCL from HC or P1. Specificity of ICOSL-based costimulation was confirmed by blocking ICOSL on LCL before coculture (αICOSL; B) or by reconstitution of WT ICOSL in LCL from HC (D). The values represent the mean ± SEM fold change in expression relative to housekeeping genes (*GAPDH*, shown; *UBASH3B*, not shown). Data represent the means from triplicates, and results are representative of at least three independent experiments. *, P < 0.032; ****, P < 0.0001.

the limited number of primary neutrophils from P1, we investigated the consequences of endothelial ICOSL deficiency on the migration of neutrophils from HCs. Surprisingly, we identified that mutant ICOSL expressed in endothelial cells significantly decreased the transmigration capacity of HC neutrophils. This defective migration occurred in response to both intermediary endogenous chemoattractants (IL-8; Fig. 6 B) and end target chemoattractants (fMLP; Fig. 6 C). To define the basis for this defect, we evaluated the effect of ICOSL on the cell-surface expression of adhesion molecules involved in neutrophil recruitment. Compared with the untransfected state, HMEC-1 cells transfected with ICOSL WT significantly increased cell-surface expression of E-selectin and ICAM-1, but not of VCAM-1; this selective effect on E-selectin and ICAM-1 was significantly di-

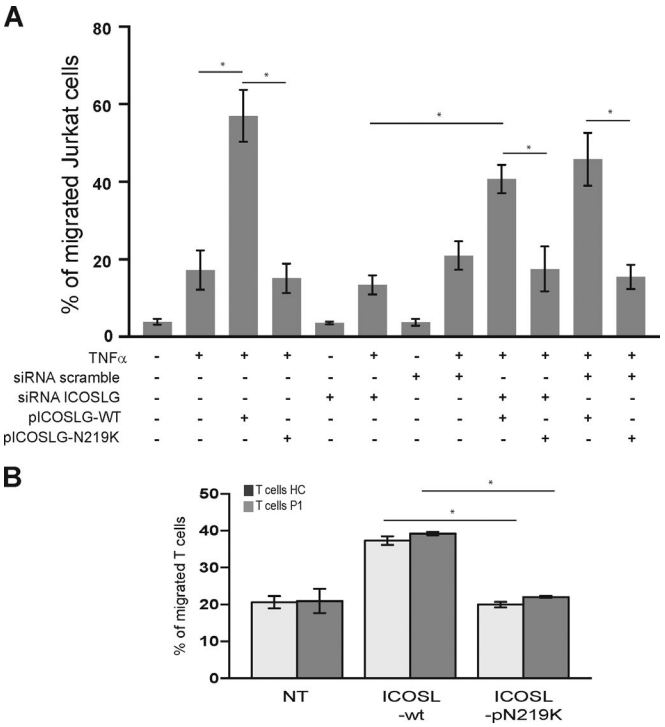

Figure 5. **Impaired ICOSL-mediated transendothelial migration of T cells.** HMEC-1 cells were silenced for endogenous ICOSL (or scramble control) and reconstituted with WT or p.N219K ICOSL. **(A and B)** TNFα was used to activate Jurkat cells (A) or primary T cells (B) isolated from P1 or HC, and frequency of T cell migration across HMEC-1 cells was measured. Data represent the means from triplicates, and results are representative of at least three independent experiments. *, $P < 0.05$.

minished with ICOSL p.N219K (Figs. 7 and S3 B). Blocking of E-selectin (Fig. S5 A) or ICAM-1 (data not shown) with respective antibody mirrored the impaired neutrophil migration seen with mutant ICOSL. The basis for the reduced E-selectin and ICAM-1 expression was not at the level of transcription, since qPCR analysis revealed no difference in induction of the respective genes (Fig. S3 C), suggesting that ICOSL may affect posttranscriptional processing of these molecules, such as the shuttling of E-selectin and ICAM-1 to the cell surface. These results implicate ICOSL on endothelial cells in the transmigration of neutrophils. This effect may provide an explanation for the neutropenia observed in the patient.

Because ICAM-1 is also required for immunological synapse formation between APCs and T cells (Dustin, 2014), and we show that ICAM-1 cell-surface expression is impaired with mutant ICOSL in HMEC-1, we assessed whether ICAM-1 expression was also reduced on P1's LCL to determine whether a similar phenomenon could account for the blunted T cell costimulation observed in the coculture assays. In P1's LCL, ICAM-1 basal cell-surface expression was robust and comparable to HCs (Fig. S4), despite the absence of ICOSL. Along with the diminished responses seen following blocking of ICOSL and the rescue of costimulatory activity with complementation of P1's LCL with WT *ICOSLG* (Fig. S5, C and D; and Fig. 4 C, respectively), this confirms the direct effect of the mutant ICOSL, but not ICAM-1, on T/APC costimulation.

Discussion

We describe here a novel CID syndrome due to autosomal recessive *ICOSLG* deficiency. ICOSL is reported to interact monogamously with its receptor, ICOS, on the surface of activated T cells (Nurieva et al., 2003). Moreover, inducible ICOSL surface expression is regulated by NIK (*MAP3K14*; Willmann et al., 2014). Indeed, the clinical features of this ICOSL-deficient patient phenocopy those seen in both ICOS and NIK deficiency, and the immunological findings mirror closely what has been reported in their respective mouse models (Table 4). All three conditions are marked by hypogammaglobulinemia with recurrent respiratory tract infections. In ICOS deficiency, this is due to impaired homeostasis of GCs resulting from the loss of ICOS-driven survival and migration signals in Tfh cells required for development of switched antibody responses and formation of memory B cells (Bossaller et al., 2006; Yong et al., 2009), whereas in NIK deficiency, there is significantly decreased B cell–surface expression of ICOSL after in vitro stimulation with CD40 Ligand (Willmann et al., 2014).

Here, in ICOSL deficiency, our costimulation model demonstrates that cytokine responses critical for high-affinity antibody production are profoundly diminished. This is expected to stunt T cell–induced B cell maturation/differentiation, explaining the observed predominance of circulating naive B cells and quasi-absence of switched memory cells. As distinct from ICOS and NIK deficiency, in which circulating total Tfh precursor cells ($CD4^+$ $CXCR5^+$) are decreased (Bossaller et al., 2006; Willmann et al., 2014; Robertson et al., 2015; Schepp et al., 2017), the circulating total Tfh precursor cell ($CD4^+$ $CXCR5^+$) population in the ICOSL-deficient patient was in the lower end of in-house reference range of controls. However, subtype analysis strikingly revealed a skewing in P1, with an elevated proportion of Tfh partial effector cells ($CD45RA^-$ $CD4^+$ $CXCR5^+$ $PD\text{-}1^{hi}$ $CCR7^{lo}$) and diminished levels of Tfh resting cells ($CD45RA^-$ $CD4^+$ $CXCR5^+$ $PD\text{-}1^{lo}$ $CCR7^{hi}$; He et al., 2013). Although all Tfh cells have an antigen-experienced phenotype ($CD45RA^-$), Tfh partial effector cells are most potent in promoting B cell differentiation within GCs for effective antibody production, whereas Tfh resting cells have a central memory phenotype with the capacity to become activated GC Tfh cells upon cognate reactivation (He et al., 2013; Schmitt and Ueno, 2013 Crotty, 2014; Hale and Ahmed, 2015). B cells have been shown to be necessary for the induction and maintenance of Tfh cells, as a result of their dual function as APCs and source of ICOSL, highlighting their symbiotic relation. In this patient, the loss of ICOSL in the B cell compartment causes ineffective T–B interactions in vitro and likely in vivo, compromising GC formation. Consequently, the Tfh cells may not be able to home properly within lymphoid organs, not only because of impaired T cell migration across mutant endothelial cells, as we have shown, but also from dysfunction of mutant follicular bystander B cells, which normally use their surface ICOSL expression to produce an "ICOS engaging field" to recruit T cells to follicles to generate a GC response, as shown in the mouse (Xu et al., 2013). In addition to improper homing into GCs, the elevated circulating Tfh partial effector cells may also result from failure of their retention within the GC (e.g., due to reduced ability to form long-term conjugates with cognate B cells) and/or increased proliferation due to lack of

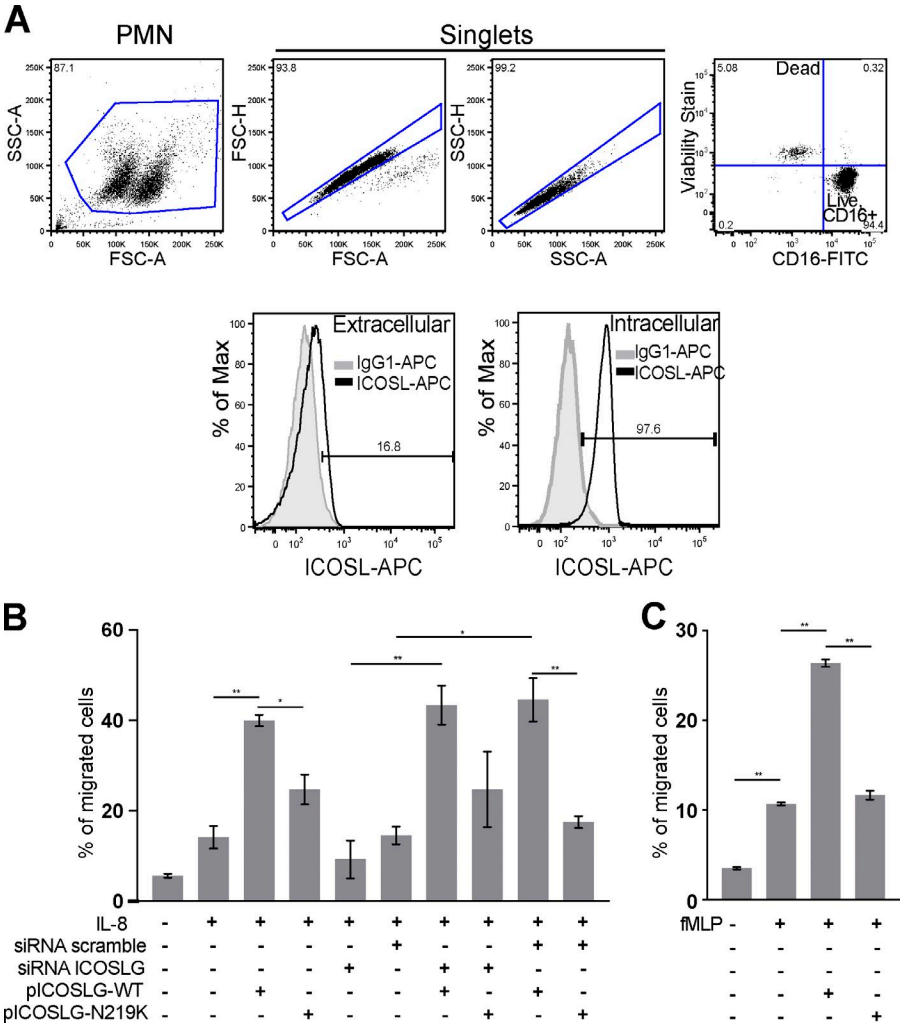

Figure 6. **Impact of ICOSL on transendothelial migration of neutrophils. (A)** ICOSL surface and intracellular protein expression in freshly isolated neutrophils. Gating strategy for CD16$^+$ live polymorphonuclear cells (PMN) shown. Histogram demonstrating ICOSL expression (dark line) relative to isotype control (shaded). **(B and C)** Migration of HC neutrophils across HMEC-1 cells, silenced for endogenous ICOSL (or scramble control) and reconstituted with WT or p.N219K ICOSLG, toward IL-8 (B) or fMLP (C). Data points represent the means from triplicates, and results are representative of three independent experiments. *, P < 0.05; **, P < 0.01.

homeostatic feedback. Identification and characterization of additional ICOSL-deficient patients will help confirm whether this Tfh skewing is a defining feature of this disorder, and whether it distinguishes ICOSL from ICOS and NIK deficiency. Collectively, these findings explain P1's lack of seroconversion to T-dependent antigens. Although the ICOSL-deficient mouse models demonstrate intact response to T-independent antigens (Wong et al., 2003), seroconversion to polysaccharide-based vaccines were not tested in the patient before starting immunoglobulin replacement (and he declined pausing it for assessment).

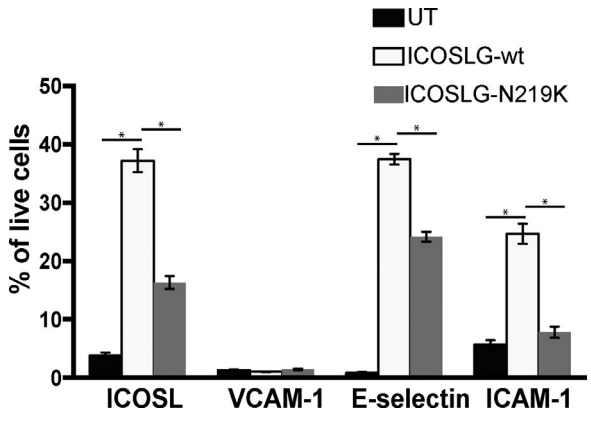

Figure 7. **Effect of ICOSL on cell-surface expression of endothelial adhesion molecules.** Cell-surface flow cytometry analysis of adhesion molecules (VCAM-1; E-selectin; ICAM-1) on live HMEC-1 cells, transfected with ICOSL WT or N219K. Data points represent the means from triplicates, and results are representative of three independent experiments. *, P < 0.05.

P1 also developed recurrent disease with microbes normally controlled by cell-mediated immunity, particularly DNA-based viruses (i.e., HPV and HSV), phenocopying some patients with ICOS deficiency (Robertson et al., 2015; Schepp et al., 2017) and NIK deficiency (Willmann et al., 2014). Although ICOS is up-regulated on activated T cells to generate the T cell–dependent B cell help described above, ICOS has also been shown to be necessary for optimal CD8$^+$ T cell proliferation and cytokine production during recall responses (Wallin et al., 2001; Takahashi et al., 2009) and, more recently in mice, activation of NK cells (Ogasawara et al., 2002) and iNKT cells (Akbari et al., 2008); these cells are implicated in immune response to viruses (Orange, 2013; Hammer et al., 2018; Rao et al., 2018). Although it has been reported that ICOS exerts negligible effect on T helper cell antiviral responses, it should be noted that this was to lymphocytic choriomeningitis virus (Kopf et al., 2000), vesicular stomatitis virus (Kopf et al., 2000), and influenza virus (Bertram et al., 2002), which are all RNA-based viruses,

Table 4. **Comparison of ICOSL, ICOS, and NIK deficiency in mouse and human**

Features	Mice			Humans		
	***ICOSLG* deficiency**	***ICOS* deficiency**	**NIK (MAP3K14) deficiency**	***ICOSLG* deficiency**	***ICOS* deficiency**	**NIK (MAP3K14) deficiency**
Infections				Recurrent respiratory tract infections	Recurrent respiratory tract infections	Recurrent respiratory tract infections
				Intestinal infections (*Campylobacter*)	Intestinal infections (*Campylobacter*, *Salmonella* norovirus, adenovirus, *Cryptosporidium*)	Intestinal infections (*Cryptosporidium*; CMV)
					Skin abscesses	Osteomyelitis with BCG
				Herpesviridae-related infections	*Herpesviridae*-related infections; recurrent HSV (labialis, keratitis, genital), CMV, HHV6	
				HPV	HPV: warts, cancer	
					Pneumocystis jiroveci pneumonia	
Other salient clinical features				Intermittent chronic diarrhea of unclear etiology (no evidence of infectious or inflammatory bowel disease)	Autoimmunity: RA, IBD, interstitial pneumonitis, psoriasis	Granulomatous hepatitis (possibly related to disseminated BCG)
				Splenomegaly	Splenomegaly	
				Dentigerous cyst	Granulomatous skin diseases	
					Cytopenia; neutropenia; thrombocytopenia (2/15 patients each)	
					Cancer: HPV vulva; LGL-T; SCC	
Immunoglobulins				Hypogammaglobulinemia of IgG, IgA, IgM	Hypogammaglobulinemia of IgG and IgA; some with low-normal IgM	Hypogammaglobulinemia of IgG, IgA; IgM low/normal/elevated
Baseline	↓ IgG1	↓ IgG1	Normal levels of IgG, IgM			
	↓ IgG2a, IgG2b, IgA	↓ IgE	↓ IgA			
		(Some mouse models had ↓ IgG2)	Normal levels of IgG1, IgG2a			
			↓ IgG2b, IgG3			
Response to vaccination	Intact response to T cell–independent antigen (based on IgM and IgG3 response to trinitrophenol-Ficoll)	Intact response to T cell–independent antigen (based on IgM and IgG3 response to trinitrophenol-Ficoll)	Poor (nearly absent) response to ovalbumin immunization			
	↓ T cell–dependent responses (based on ↓ IgG1, ↓ IgE)	↓ T cell–dependent responses (based on ↓ IgG1, ↓ IgG2a, ↓ IgE)				

Table 4. **Comparison of ICOSL, ICOS, and NIK deficiency in mouse and human *(Continued)***

Features	Mice			Humans		
	***ICOSLG* deficiency**	***ICOS* deficiency**	**NIK (MAP3K14) deficiency**	***ICOSLG* deficiency**	***ICOS* deficiency**	**NIK (MAP3K14) deficiency**
Lymphocytes	No effect on T or B cell development from thymus or bone marrow	No effect on T or B cell development from thymus or bone marrow	Thymus: no effect on T cells	Circulating absolute T cell counts: decreased	Circulating absolute T cell counts: normal	Circulating absolute T cell counts: normal
				Circulating $CD4^+$ T cell subset: decreased	Circulating $CD4^+$ T cell subset: variable	Circulating $CD4^+$ T cell subset: normal
	No effect on overall composition of mature B and T cell subsets in spleen	No effect on overall composition of mature B and T cell subsets in spleen	Spleen: no effect on T cells; decreased $B220^+$ IgM^+ cells	Circulating $CD8^+$ T cell subset: decreased	Circulating $CD8^+$ T cell subset: variable	Circulating $CD8^+$ T cell subset: normal
				Memory T cell counts: decreased	Memory T cell counts: variable	Memory T cell counts: normal
			Bone marrow: increased $B220^+$ $CD25^+$ and $B220^+$ $CD43^-$	Circulating Tfh ($CD4^+$ $CXCR5^+$ $CD45RA$): low–normal	Reduction in circulating Tfh (defined as $CD4^+$ $CXCR5^+$ $CD45RA^-$)	Reduction in circulating Tfh ($CD4^+$ $CXCR5^+$ $CD45RA^-$)
				T reg cells: normal	T reg cells: normal	T reg cells: normal
				B cell counts: decreased in childhood; intermittently within reference range in adulthood	B cell counts: normal when diagnosed in childhood; decreased when diagnosed in adulthood	B cell counts: decreased
				Circulating naive B cells: increased	Circulating naive B cells: high (children); decreased (adults)	Circulating naive B cells: high (children)
				Circulating switched memory B cell cells: decreased	Circulating switched memory B cell cells: decreased	Circulating switched memory B cell cells: decreased
						NK cell counts: decreased
Lymphoid organs	↓ number and size of GC formation	↓ number and size of GC formation	Absent lymph nodes; abnormal lymphoid architecture in thymus and spleen			
Myeloid cells	Not reported	Not reported	↓ $CD11b^+$ monocytes in spleen	Progressive neutropenia	Neutropenia (n = 2)	Not reported

The immunological findings in the mouse (top) and clinical features in humans (bottom) are listed. BCG, Bacillus Calmette-Guérin; RA, rheumatoid arthritis; IBD, inflammatory bowel disease; LGL-T, large granular lymphocyte T cells; SCC, squamous cell carcinoma.

whereas the problematic viral diseases reported in humans with compromised ICOS:ICOSL axis have been DNA-based (Table 4).

Intriguingly, NK cells are persistently decreased in both NIK deficiency (Willmann et al., 2014) and this ICOSL-deficient patient. Given the importance of NK cells in immunity to DNA-based viruses identified in other inborn errors of immunity (Vinh et al., 2010; Orange, 2013), it would be important to evaluate the NK compartment in ICOS deficiency to guide further studies on the role of the ICOS:ICOSL axis in NK biology. Although the circulating classical DC compartment was quantitatively similar between P1 and controls, it has been previously shown that ICOSL is up-regulated on activated DCs, enhancing allostimulation of T cells and generation of a Th1 response (Richter et al., 2001; Liang et al., 2002). We are currently exploring the ICOSL-mediated mechanisms of antiviral immunity.

In addition to APCs, ICOSL is broadly distributed. It is expressed on endothelial cells, fibroblasts, and renal epithelial cells (Swallow et al., 1999; Khayyamian et al., 2002). Deficiency in these nonhematopoietic cell types may further contribute to the clinical features observed in P1. Indeed, our data demonstrate that ICOSL deficiency on endothelial cells (HMEC-1) results in defective T cell transmigration; this effect was observed with both

Jurkat cells and primary T lymphocytes from P1 and controls, excluding a T cell–intrinsic defect in the patient and ascribing the phenomenon to an endothelial process. HMEC-1 is the prototypical human microvascular endothelial cell line, representing the microvascular compartment in both lymphoid and nonlymphoid tissues through which leukocytes home (Ades et al., 1992). The diminished ability of T cells to migrate across mutant-transfected HMEC-1 may reflect impaired trafficking within lymphoid organs in vivo, working in conjunction with blunted cell–cell costimulation to further compromise antibody responses.

Our transmigration model also identified a novel role for endothelial ICOSL in the regulation of cell-surface expression of E-selectin and ICAM-1. Although E-selectin on postcapillary venules contributes to the rolling of leukocytes at sites of inflammation and tissue injury, the mouse model suggests redundancy in this function, as E-selectin knockout mice have no defect in leukocyte recruitment to inflamed tissue unless P-selectin is simultaneously blocked (Frenette et al., 1996; Malý et al., 1996). This redundancy in neutrophil recruitment may account for the lack of significant disease typically associated with circulating neutropenia in P1. Interestingly, E-selectin plays a key role for homing of T cells to the skin (Kansas, 1996), which may contribute to the persistent warts. On the other hand, E-selectin is highly expressed on bone marrow vascular endothelium (Jacobsen et al., 1996; Schweitzer et al., 1996), and recent data demonstrate a distinct role in this niche: E-selectin expression is required for hematopoietic stem cell (HSC) proliferation, whereas E-selectin deficiency leads to HSC quiescence with greater capacity for self-renewal (Winkler et al., 2012). This ICOSL-mediated effect on adhesion molecules may explain the normocellular marrow with circulating neutropenia in P1. It may also account for the rare development of neutropenia in patients with ICOS deficiency, which appears to be autoimmune in basis (Warnatz et al., 2006; Schepp et al., 2017). Thus, our findings in this ICOSL-deficient patient may reflect a dysfunction in neutrophil egress from the bone marrow into the circulation, dysregulated marginalization in the vasculature, or even potentially altered neutrophil cell survival. The exact basis by which loss of ICOSL produces neutropenia requires further elucidation. Moreover, the molecules mediating downstream signaling of ICOSL, and whether distinct signal transduction pathways are used by specific ICOSL-expressing cells, remain to be deciphered.

The recessive p.N219K mutation locates to the IgC domain of the extracellular region of ICOSL. Chattopadhyay et al. (2006) have shown that the IgC domain is required to form nonconvalent homodimers, loss of which causes ICOSL to form nonspecific aggregates. Our in silico analyses suggest that P1's mutation results in loss of form in this domain (via gain of a pure coil arrangement) with decreased rigidity, which likely affects the capacity of ICOSL to assume its proper structure for further processing. Our confocal microscopy findings are consistent with this abnormal conformation, demonstrating retention of mutant protein in the ER-Golgi apparatus. The significant gain in hydrophilicity likely further compromises its processing, by impeding its translocation across lipid membranes, which is a catastrophic alteration for single-pass type I membrane proteins such as ICOSL. In keeping with these significant biochemical alterations, maneuvers to attempt to rescue the defect, such as variation in ambient temperature, cytokine stimulation, and inhibitors of discrete pathways of protein degradation, did not result in increased expression of cell-surface protein. Although the exact molecular pathways of ICOSL signaling are undefined, the loss of form imparted by N219K, causing a loss of surface expression and loss of cellular function, is consistent with the recessive nature of the disease.

Most patients with ICOS deficiency have been treated with supportive care. Recently, the experience of HSC transplant on three such patients has been reported, with a fatal HSC transplant–related outcome in one (Schepp et al., 2017). However, given the broader nonhematopoietic cellular distribution of ICOSL, and our data demonstrating that at least some of the clinical manifestations may relate to deficiency on these latter cell types, there should be caution about the interchangeability of the management of these two conditions; this also applies to therapies targeting the ICOS:ICOSL axis. Our discovery and characterization of ICOSL deficiency provides the basis for future studies to characterize the full clinical and immunological phenotype, as well as optimal management strategies, of this novel inborn error of immunity.

Materials and methods

Subjects

Subjects and the patient's family members provided informed consent on McGill University Health Centre (MUHC) institutional review board–approved research protocol (GEN10-256). Comprehensive medical histories, including review of all available outside records and serial clinical evaluations, as well as clinical immunological laboratory testing, were performed at the MUHC.

Sequencing and bioinformatics analysis

WES was performed as previously done (Gavino et al., 2017). Briefly, exome enrichment was conducted on genomic DNA (gDNA) sample library using the SeqCap EZ Exome v3+ UTR library (64 Mb sequence capture) from Roche-Nimblegen. The enriched gDNA fragments were sequenced (PE100) on an Illumina HiSeq 2000. The WES data were analyzed following the GATK Best Practices recommendations for variant discovery in DNA-Seq, with GATK version 3 (Andrews, 2010; Li and Durbin, 2010; McKenna et al., 2010; DePristo et al., 2011 Cingolani et al., 2012a,b; Van Der Auwera et al., 2013). After verifying the quality of the reads with FastQC (Andrews, 2010), the reads were aligned with the Burrows-Wheeler Aligner (v0.7.12-r1039; Li and Durbin, 2010) to the GRCh37 reference genome. Duplicate reads were marked with Picard tools. Reads were realigned around indels with GATK IndelRealigner. Base quality scores were recalibrated with GATK BaseRecalibrator. Variant calling was performed with GATK HaplotypeCaller. Variant annotation was perfomed with SnpSift (Cingolani et al., 2012a) and SnpEff (Cingolani et al., 2012b). Only variants with coverage of at least 10 reads were kept for downstream analysis. To identify rare variants, the frequency of the variants in the Exome Aggregation Consortium (Lek et al., 2016) database was reported.

For Sanger sequencing, the *ICOSLG* gene was PCR amplified from genomic DNA using primers designed to flank the respective regions (primers and sequencing conditions available on re-

quest). Sequencing was performed at the McGill University and Génome Québec Innovation Centre. Sequencing analyses were performed on Sequencher sequence analysis software (Gene Codes Corporation). Potential splice sites were predicted using the online tool Human Splicing Finder.

Availability of data and material

WES data are available in the National Center for Biotechnology Information Sequence Read Archive database under accession no. PRJNA497908 (project ID SUB4666846).

Cell culture

Immortalized human dermal microvascular endothelium HMEC-1 cells were purchased from ATCC (CRL-3243) and cultured in MCDB 131 medium containing 10 ng/ml epidermal growth factor, 1 µg/ml hydrocortisone, 10 mM glutamine, and 10% FBS. LCLs were established as previously described (Vinh et al., 2011; Gavino et al., 2014, 2016). LCLs and Jurkat were cultured in RPMI supplemented with 10% FBS, 20 mM Hepes, and antibiotics. T cells were isolated ($CD3^+$ cells) directly from human peripheral blood mononuclear cells by immunomagnetic negative selection or FACS.

Antibodies

Anti-ICOSL (MIH12), ICOSL-APC, CD16-PE, anti–VCAM-1-PE, anti–E-Selectin-PE, CD27-PE, CD19-APC, CD45-PerCP/Cy5.5, goat anti-rabbit Alexa Fluor 488, goat anti-mouse Alexa Fluor 633, and Alexa Fluor 568 were from Thermo Fisher Scientific. CD19-FITC, IgD-FITC, FoxP3-A647, CD14-FITC, and CD45RA-PE were from BD Biosciences. Antibodies against RCAS1 and β-actin were from Cell Signaling Technology. HLA-DR-PerCP, CD11c-Pacific Blue, CXCR5-BV421, CCR7-APC/Cy7, PD1-PE/Cy7, and ICOS-APC were from BioLegend. BDCA1 (CD1c)-APC, BDCA3 (CD141)-PE, CD4-FITC, and ICAM-1-FITC were from R&D Systems.

DNA constructs and transfection

The Myc-flag tagged WT *ICOSLG* plasmid was purchased from OriGene. The WT *ICOSLG* plasmid was used to create the p.N219K mutant using site-directed mutagenesis kit (New England Biolabs). HMEC-1 were electroporated with by Amaxa Nucleofector Technology (Lonza) for 24 h. Duplex siRNA against *ICOSLG* or universal scrambled siRNA were purchased from OriGene (locus ID 23308, R308174). Transient transfection of HMEC-1 with 10 nM siRNAs was performed using Lipofectamine RNAiMAX (Invitrogen) according to the manufacturer's instructions.

Confocal microscopy

Cells were fixed in 2% PFA, permeabilized in 2% saponin, and stained with antibodies as indicated. LIVE/DEAD Fixable Cell Stain Kit (Thermo Fisher Scientific) was used per the manufacturer's instructions. Images were acquired using a Zeiss LSM780 Laser scanning confocal microscope and Zen2010 software (Carl Zeiss).

Coculture experiments

Cocultured Jurkat cells were pretreated with TNFα (50 ng/ml, 2 h) with EBV-LCL from HC or P1. The contribution of ICOSL was determined by the addition of ICOSL neutralizing Ab (10 µg/ml, 2 h) as indicated. After 24 h of coculture, total RNA was isolated and reverse transcribed with the Maxima cDNA synthesis kit for RT-qPCR (Thermo Fisher Scientific). Quantitative real-time PCR was performed using the Taqman qPCR Gene Expression assay system (Thermo Fisher Scientific) on the Applied Biosystem 7300 real-time PCR system. The mRNA input was normalized to the expression of the housekeeping genes, *GAPDH* or *UBASH3B* (Gavino et al., 2017). Statistical significance of the data was validated using one-way ANOVA with Tukey's post hoc test and multiple comparison procedure. The level of significance was set at *, $P < 0.032$, and ****, $P < 0.0001$.

Transendothelial cell migration assay

HMEC-1 were grown to confluence for 48 h on 5.0-µm pore size gelatinized polycarbonate membranes of modified Boyden chambers (Transwell, Thermo Fisher Scientific). Neutrophils or Jurkat cells were left in suspension for 1 h before being labeled for 30 min with calcein AM (0.5 µM) and washed with HBSS buffer. Thereafter, HMEC-1 were transfected with SiRNA against ICOSLG for 48 h, then electroporated with ICOSLG-wt or ICOSLG-pN219K for 24 h, and finally washed with HBSS buffer. Neutrophils or Jurkat cells (500,000) were added for 5 h in the upper chamber. As a chemoattractant for polymorphonuclear cells, IL-8 (10 ng/ml), and for Jurkat, CXCL12/SDF-1α (25 ng/ml; R&D Systems) were used and applied in the lower compartment of the Transwell filter. Transwells were incubated at 37°C in a humidified incubator with 5% CO_2 (6 h for Jurkat and 2 h for neutrophils), and migration of cells through the endothelium was detected using fluorescent plate reader (Tecan M1000). The migration ratio was calculated with the following formula: [total number of migrated calcein AM–labeled cells/total number of input calcein-AM-labeled cells] × 100. Data points represent the means from triplicates, and results are representative of three independent experiments. For statistical analysis, repeated-measures one-way ANOVA followed by Tukey's multiple comparison post-test was used. The level of significance was set at *, $P < 0.05$.

Flow cytometry

Cells were blocked in Fc Receptor Binding Inhibitor Monoclonal Antibody and incubated with LIVE/DEAD Fixable Dead Cell Stain (Thermo Fisher Scientific). Cells were stained using the FIX & PERM Cell Fixation and Cell Permeabilization Kit (Thermo Fisher Scientific). For the immunophenotyping, 100 µl blood was incubated with appropriate antibodies for 30 min at room temperature. Red cell lysis was performed with FACS Lysing Solution (BD Biosciences) according to the manufacturer's recommendations. Samples were run on the BD FACSCanto II, and data were acquired using BD FACSDIVA software (BD Biosciences). Data were analyzed using FlowJo.

Online supplemental material

Fig. S1 shows flow cytometry gating strategy for immunophenotyping of P1. Fig. S2 shows conformational and biochemical analyses of ICOSL p.N219K. Fig. S3 shows the effect of $ICOSL^{N219K}$ in reconstituted HMEC-1 cells. Fig. S4 shows ICAM1 expression in lymphoblastoid cells. Fig. S5 shows the effect of ICOSL on E-selectin–mediated transendothelial migration of neutrophils. Table S1 lists variant calling statistics for WES of P1.

Acknowledgments

We thank the patient and his family for their participation. We thank the interdisciplinary medical personnel involved in the care of the patient and his family.

A. Veillette holds the Canada Research Chair in Signaling in the Immune System and is supported by a grant from the Canadian Institutes of Health Research (FDN-143338). He has a contract from Bristol-Myers Squibb to study the mechanism of action of anti-SLAMF7 monoclonal antibody elotuzumab. D.C. Vinh is supported by Fonds de Recherche du Québec - Santé Chercheur boursier clinicien Junior 2 salary award. This work was supported by research funds from La Fondation du Grand Défi Pierre Lavoie, Research Institute–McGill University Health Centre (Merck, Sharpe & Dohme award), and CSL Behring Canada.

D.C. Vinh has received research support, unrestricted educational grants, consultancy fees, and speaker honoraria from CSL Behring Canada; has received consultancy fees from Astellas Canada, Avir Pharma, Novartis Canada, and Shire Canada; and has undertaken clinical trials for Cidara Therapeutics and CSL Behring. The remaining authors declare no competing financial interests.

Author contributions: L. Roussel designed and performed the experiments, analyzed and interpreted data, wrote the paper, and prepared the figures. M. Landekic, C. Gavino, M.-C. Zhong, J. Chen, D. Faubert, J. Luo, C. Le, B.R. Ford, I.L. King, and M. Divangahi performed the experiments and analyzed and interpreted the data. A. Blanchet-Cohen analyzed the WES data and submitted it to GEO. W.D. Foulkes assisted in analyzing the genetics data. M. Golizeh performed the biochemical protein analysis. L. Dansereau, M.A. Parent, S. Marin, and M. Langelier collected the clinical materials and data. M.-C. Zhong, J. Chen, and A. Veillette provided custom reagents. A. Veillette and D.C. Vinh supervised the research and revised the manuscript. D.C. Vinh designed the experiments, supervised the research, analyzed and interpreted the data, and wrote the paper.

Submitted: 9 April 2018
Revised: 21 September 2018
Accepted: 6 November 2018

References

Ades, E.W., F.J. Candal, R.A. Swerlick, V.G. George, S. Summers, D.C. Bosse, and T.J. Lawley. 1992. HMEC-1: establishment of an immortalized human microvascular endothelial cell line. *J. Invest. Dermatol.* 99:683–690. https://doi.org/10.1111/1523-1747.ep12613748

Afzali, B., J. Grönholm, J. Vandrovcova, C. O'Brien, H.W. Sun, I. Vanderleyden, F.P. Davis, A. Khoder, Y. Zhang, A.N. Hegazy, et al. 2017. BACH2 immunodeficiency illustrates an association between super-enhancers and haploinsufficiency. *Nat. Immunol.* 18:813–823. https://doi.org/10.1038/ni.3753

Akbari, O., P. Stock, E.H. Meyer, G.J. Freeman, A.H. Sharpe, D.T. Umetsu, and R.H. DeKruyff. 2008. ICOS/ICOSL interaction is required for CD4+ invariant NKT cell function and homeostatic survival. *J. Immunol.* 180:5448–5456. https://doi.org/10.4049/jimmunol.180.8.5448

Andrews, S.2010. FastQC A Quality Control tool for High Throughput Sequence Data. http://www.bioinformatics.babraham.ac.uk/projects/fastqc/. Accessed May 16, 2016.

Bertram, E.M., A. Tafuri, A. Shahinian, V.S. Chan, L. Hunziker, M. Recher, P.S. Ohashi, T.W. Mak, and T.H. Watts. 2002. Role of ICOS versus CD28 in antiviral immunity. *Eur. J. Immunol.* 32:3376–3385. https://doi.org/10.1002/1521-4141(200212)32:12%3C3376::AID-IMMU3376%3E3.0.CO;2-Y

Bossaller, L., J. Burger, R. Draeger, B. Grimbacher, R. Knoth, A. Plebani, A. Durandy, U. Baumann, M. Schlesier, A.A. Welcher, et al. 2006. ICOS deficiency is associated with a severe reduction of CXCR5+CD4 germinal center Th cells. *J. Immunol.* 177:4927–4932. https://doi.org/10.4049/jimmunol.177.7.4927

Casanova, J.L., and L. Abel. 2018. Human genetics of infectious diseases: Unique insights into immunological redundancy. *Semin. Immunol.* 36:1–12. https://doi.org/10.1016/j.smim.2017.12.008

Chattopadhyay, K., S. Bhatia, A. Fiser, S.C. Almo, and S.G. Nathenson. 2006. Structural basis of inducible costimulator ligand costimulatory function: determination of the cell surface oligomeric state and functional mapping of the receptor binding site of the protein. *J. Immunol.* 177:3920–3929. https://doi.org/10.4049/jimmunol.177.6.3920

Cingolani, P., V.M. Patel, M. Coon, T. Nguyen, S.J. Land, D.M. Ruden, and X. Lu. 2012a. Using Drosophila melanogaster as a Model for Genotoxic Chemical Mutational Studies with a New Program, SnpSift. *Front. Genet.* 3:35. https://doi.org/10.3389/fgene.2012.00035

Cingolani, P., A. Platts, L. Wang, M. Coon, T. Nguyen, L. Wang, S.J. Land, X. Lu, and D.M. Ruden. 2012b. A program for annotating and predicting the effects of single nucleotide polymorphisms, SnpEff: SNPs in the genome of Drosophila melanogaster strain w1118; iso-2; iso-3. *Fly (Austin).* 6:80–92. https://doi.org/10.4161/fly.19695

Crotty, S. 2014. T follicular helper cell differentiation, function, and roles in disease. *Immunity.* 41:529–542. https://doi.org/10.1016/j.immuni.2014.10.004

DePristo, M.A., E. Banks, R. Poplin, K.V. Garimella, J.R. Maguire, C. Hartl, A.A. Philippakis, G. del Angel, M.A. Rivas, M. Hanna, et al. 2011. A framework for variation discovery and genotyping using next-generation DNA sequencing data. *Nat. Genet.* 43:491–498. https://doi.org/10.1038/ng.806

Dotta, L., and R. Badolato. 2014. Primary immunodeficiencies appearing as combined lymphopenia, neutropenia, and monocytopenia. *Immunol. Lett.* 161:222–225. https://doi.org/10.1016/j.imlet.2013.11.018

Dustin, M.L. 2014. The immunological synapse. *Cancer Immunol. Res.* 2:1023–1033. https://doi.org/10.1158/2326-6066.CIR-14-0161

Frenette, P.S., T.N. Mayadas, H. Rayburn, R.O. Hynes, and D.D. Wagner. 1996. Susceptibility to infection and altered hematopoiesis in mice deficient in both P- and E-selectins. *Cell.* 84:563–574. https://doi.org/10.1016/S0092-8674(00)81032-6

Gavino, C., A. Cotter, D. Lichtenstein, D. Lejtenyi, C. Fortin, C. Legault, N. Alirezaie, J. Majewski, D.C. Sheppard, M.A. Behr, et al. 2014. CARD9 deficiency and spontaneous central nervous system candidiasis: complete clinical remission with GM-CSF therapy. *Clin. Infect. Dis.* 59:81–84. https://doi.org/10.1093/cid/ciu215

Gavino, C., N. Hamel, J.B. Zeng, C. Legault, M.C. Guiot, J. Chankowsky, D. Lejtenyi, M. Lemire, I. Alarie, S. Dufresne, et al. 2016. Impaired RASGRF1/ERK-mediated GM-CSF response characterizes CARD9 deficiency in French-Canadians. *J. Allergy Clin. Immunol.* 137:1178–1188.e7. https://doi.org/10.1016/j.jaci.2015.09.016

Gavino, C., M. Landekic, J. Zeng, N. Wu, S. Jung, M.C. Zhong, A. Cohen-Blanchet, M. Langelier, O. Neyret, D. Lejtenyi, et al. 2017. Morpholino-based correction of hypomorphic ZAP70 mutation in an adult with combined immunodeficiency. *J. Allergy Clin. Immunol.* 139:1688–1692.e10. https://doi.org/10.1016/j.jaci.2017.02.002

Grimbacher, B., A. Hutloff, M. Schlesier, E. Glocker, K. Warnatz, R. Dräger, H. Eibel, B. Fischer, A.A. Schäffer, H.W. Mages, et al. 2003. Homozygous loss of ICOS is associated with adult-onset common variable immunodeficiency. *Nat. Immunol.* 4:261–268. https://doi.org/10.1038/ni902

Hale, J.S., and R. Ahmed. 2015. Memory T follicular helper CD4 T cells. *Front. Immunol.* 6:16. https://doi.org/10.3389/fimmu.2015.00016

Hammer, Q., T. Rückert, and C. Romagnani. 2018. Natural killer cell specificity for viral infections. *Nat. Immunol.* 19:800–808. https://doi.org/10.1038/s41590-018-0163-6

He, J., L.M. Tsai, Y.A. Leong, X. Hu, C.S. Ma, N. Chevalier, X. Sun, K. Vandenberg, S. Rockman, Y. Ding, et al. 2013. Circulating precursor CCR7(lo)PD-1(hi) CXCR5$^+$ CD4$^+$ T cells indicate Tfh cell activity and promote antibody responses upon antigen reexposure. *Immunity.* 39:770–781. https://doi.org/10.1016/j.immuni.2013.09.007

Hutloff, A., A.M. Dittrich, K.C. Beier, B. Eljaschewitsch, R. Kraft, I. Anagnostopoulos, and R.A. Kroczek. 1999. ICOS is an inducible T-cell co-stimulator structurally and functionally related to CD28. *Nature.* 397:263–266. https://doi.org/10.1038/16717

Jacobsen, K., J. Kravitz, P.W. Kincade, and D.G. Osmond. 1996. Adhesion receptors on bone marrow stromal cells: in vivo expression of vascular cell adhesion molecule-1 by reticular cells and sinusoidal endothelium in normal and gamma-irradiated mice. *Blood.* 87:73–82.

Kansas, G.S. 1996. Selectins and their ligands: current concepts and controversies. *Blood.* 88:3259–3287.

Khayyamian, S., A. Hutloff, K. Büchner, M. Gräfe, V. Henn, R.A. Kroczek, and H.W. Mages. 2002. ICOS-ligand, expressed on human endothelial cells, costimulates Th1 and Th2 cytokine secretion by memory CD4+ T cells. *Proc. Natl. Acad. Sci. USA.* 99:6198–6203. https://doi.org/10.1073/pnas.092576699

Kopf, M., A.J. Coyle, N. Schmitz, M. Barner, A. Oxenius, A. Gallimore, J.C. Gutierrez-Ramos, and M.F. Bachmann. 2000. Inducible costimulator protein (ICOS) controls T helper cell subset polarization after virus and parasite infection. *J. Exp. Med.* 192:53–61. https://doi.org/10.1084/jem.192.1.53

Lagresle-Peyrou, C., S. Luce, F. Ouchani, T.S. Soheili, H. Sadek, M. Chouteau, A. Durand, I. Pic, J. Majewski, C. Brouzes, et al. 2016. X-linked primary immunodeficiency associated with hemizygous mutations in the moesin (MSN) gene. *J. Allergy Clin. Immunol.* 138:1681–1689.e8. https://doi.org/10.1016/j.jaci.2016.04.032

Lek, M., K.J. Karczewski, E.V. Minikel, K.E. Samocha, E. Banks, T. Fennell, A.H. O'Donnell-Luria, J.S. Ware, A.J. Hill, B.B. Cummings, et al. Exome Aggregation Consortium. 2016. Analysis of protein-coding genetic variation in 60,706 humans. *Nature.* 536:285–291. https://doi.org/10.1038/nature19057

Li, H., and R. Durbin. 2010. Fast and accurate long-read alignment with Burrows-Wheeler transform. *Bioinformatics.* 26:589–595. https://doi.org/10.1093/bioinformatics/btp698

Liang, L., E.M. Porter, and W.C. Sha. 2002. Constitutive expression of the B7h ligand for inducible costimulator on naive B cells is extinguished after activation by distinct B cell receptor and interleukin 4 receptor-mediated pathways and can be rescued by CD40 signaling. *J. Exp. Med.* 196:97–108. https://doi.org/10.1084/jem.20020298

Malý, P., A. Thall, B. Petryniak, C.E. Rogers, P.L. Smith, R.M. Marks, R.J. Kelly, K.M. Gersten, G. Cheng, T.L. Saunders, et al. 1996. The alpha(1,3)fucosyltransferase Fuc-TVII controls leukocyte trafficking through an essential role in L-, E-, and P-selectin ligand biosynthesis. *Cell.* 86:643–653. https://doi.org/10.1016/S0092-8674(00)80137-3

McKenna, A., M. Hanna, E. Banks, A. Sivachenko, K. Cibulskis, A. Kernytsky, K. Garimella, D. Altshuler, S. Gabriel, M. Daly, and M.A. DePristo. 2010. The Genome Analysis Toolkit: a MapReduce framework for analyzing next-generation DNA sequencing data. *Genome Res.* 20:1297–1303. https://doi.org/10.1101/gr.107524.110

Mowen, K.A., and M. David. 2014. Unconventional post-translational modifications in immunological signaling. *Nat. Immunol.* 15:512–520. https://doi.org/10.1038/ni.2873

Notarangelo, L.D. 2014. Combined immunodeficiencies with nonfunctional T lymphocytes. *Adv. Immunol.* 121:121–190. https://doi.org/10.1016/B978-0-12-800100-4.00004-0

Nurieva, R.I., X.M. Mai, K. Forbush, M.J. Bevan, and C. Dong. 2003. B7h is required for T cell activation, differentiation, and effector function. *Proc. Natl. Acad. Sci. USA.* 100:14163–14168. https://doi.org/10.1073/pnas.2335041100

Ogasawara, K., S.K. Yoshinaga, and L.L. Lanier. 2002. Inducible costimulator costimulates cytotoxic activity and IFN-gamma production in activated murine NK cells. *J. Immunol.* 169:3676–3685. https://doi.org/10.4049/jimmunol.169.7.3676

Orange, J.S. 2013. Natural killer cell deficiency. *J. Allergy Clin. Immunol.* 132:515–525. https://doi.org/10.1016/j.jaci.2013.07.020

Picard, C., H. Bobby Gaspar, W. Al-Herz, A. Bousfiha, J.L. Casanova, T. Chatila, Y.J. Crow, C. Cunningham-Rundles, A. Etzioni, J.L. Franco, et al. 2018. International Union of Immunological Societies: 2017 Primary Immunodeficiency Diseases Committee Report on Inborn Errors of Immunity. *J. Clin. Immunol.* 38:96–128. https://doi.org/10.1007/s10875-017-0464-9

Rao, P., X. Wen, J.H. Lo, S. Kim, X. Li, S. Chen, X. Feng, O. Akbari, and W. Yuan. 2018. Herpes simplex virus-1 specifically targets human CD1d antigen presentation to enhance its pathogenicity. *J. Virol.* 92:JVI.01490-18. https://doi.org/10.1128/JVI.01490-18

Richter, G., M. Hayden-Ledbetter, M. Irgang, J.A. Ledbetter, J. Westermann, I. Körner, K. Daemen, E.A. Clark, A. Aicher, and A. Pezzutto. 2001. Tumor necrosis factor-alpha regulates the expression of inducible costimulator receptor ligand on CD34(+) progenitor cells during differentiation into antigen presenting cells. *J. Biol. Chem.* 276:45686–45693. https://doi.org/10.1074/jbc.M108509200

Robertson, N., K.R. Engelhardt, N.V. Morgan, D. Barge, A.J. Cant, S.M. Hughes, M. Abinun, Y. Xu, M.S. Koref, P.D. Arkwright, and S. Hambleton. 2015. Astute Clinician Report: A Novel 10 bp Frameshift Deletion in Exon 2 of ICOS Causes a Combined Immunodeficiency Associated with an Enteritis and Hepatitis. *J. Clin. Immunol.* 35:598–603. https://doi.org/10.1007/s10875-015-0193-x

Salzer, U., A. Maul-Pavicic, C. Cunningham-Rundles, S. Urschel, B.H. Belohradsky, J. Litzman, A. Holm, J.L. Franco, A. Plebani, L. Hammarstrom, et al. 2004. ICOS deficiency in patients with common variable immunodeficiency. *Clin. Immunol.* 113:234–240. https://doi.org/10.1016/j.clim.2004.07.002

Schepp, J., J. Chou, A. Skrabl-Baumgartner, P.D. Arkwright, K.R. Engelhardt, S. Hambleton, T. Morio, E. Röther, K. Warnatz, R. Geha, and B. Grimbacher. 2017. 14 Years after Discovery: Clinical Follow-up on 15 Patients with Inducible Co-Stimulator Deficiency. *Front. Immunol.* 8:964. https://doi.org/10.3389/fimmu.2017.00964

Schmitt, N., and H. Ueno. 2013. Blood Tfh cells come with colors. *Immunity.* 39:629–630. https://doi.org/10.1016/j.immuni.2013.09.011

Schweitzer, K.M., A.M. Dräger, P. van der Valk, S.F. Thijsen, A. Zevenbergen, A.P. Theijsmeijer, C.E. van der Schoot, and M.M. Langenhuijsen. 1996. Constitutive expression of E-selectin and vascular cell adhesion molecule-1 on endothelial cells of hematopoietic tissues. *Am. J. Pathol.* 148:165–175.

Swallow, M.M., J.J. Wallin, and W.C. Sha. 1999. B7h, a novel costimulatory homolog of B7.1 and B7.2, is induced by TNFalpha. *Immunity.* 11:423–432. https://doi.org/10.1016/S1074-7613(00)80117-X

Takahashi, N., K. Matsumoto, H. Saito, T. Nanki, N. Miyasaka, T. Kobata, M. Azuma, S.K. Lee, S. Mizutani, and T. Morio. 2009. Impaired CD4 and CD8 effector function and decreased memory T cell populations in ICOS-deficient patients. *J. Immunol.* 182:5515–5527. https://doi.org/10.4049/jimmunol.0803256

Van Der Auwera, G.A., M.O. Carneiro, C. Hartl, R. Poplin, G. Del Angel, A. Levy-Moonshine, T. Jordan, K. Shakir, D. Roazen, J. Thibault, et al.2013. From FastQ data to high confidence variant calls: the Genome Analysis Toolkit best practices pipeline. Curr. Protoc. Bioinformatics. 43:11.10.1–33.

Vinh, D.C., S.Y. Patel, G. Uzel, V.L. Anderson, A.F. Freeman, K.N. Olivier, C. Spalding, S. Hughes, S. Pittaluga, M. Raffeld, et al. 2010. Autosomal dominant and sporadic monocytopenia with susceptibility to mycobacteria, fungi, papillomaviruses, and myelodysplasia. *Blood.* 115:1519–1529. https://doi.org/10.1182/blood-2009-03-208629

Vinh, D.C., B. Schwartz, A.P. Hsu, D.J. Miranda, P.A. Valdez, D. Fink, K.P. Lau, D. Long-Priel, D.B. Kuhns, G. Uzel, et al. 2011. Interleukin-12 receptor β1 deficiency predisposing to disseminated Coccidioidomycosis. *Clin. Infect. Dis.* 52:e99–e102. https://doi.org/10.1093/cid/ciq215

Wallin, J.J., L. Liang, A. Bakardjiev, and W.C. Sha. 2001. Enhancement of CD8+ T cell responses by ICOS/B7h costimulation. *J. Immunol.* 167:132–139. https://doi.org/10.4049/jimmunol.167.1.132

Warnatz, K., L. Bossaller, U. Salzer, A. Skrabl-Baumgartner, W. Schwinger, M. van der Burg, J.J. van Dongen, M. Orlowska-Volk, R. Knoth, A. Durandy, et al. 2006. Human ICOS deficiency abrogates the germinal center reaction and provides a monogenic model for common variable immunodeficiency. *Blood.* 107:3045–3052. https://doi.org/10.1182/blood-2005-07-2955

Willmann, K.L., S. Klaver, F. Doğu, E. Santos-Valente, W. Garncarz, I. Bilic, E. Mace, E. Salzer, C.D. Conde, H. Sic, et al. 2014. Biallelic loss-of-function mutation in NIK causes a primary immunodeficiency with multifaceted aberrant lymphoid immunity. *Nat. Commun.* 5:5360. https://doi.org/10.1038/ncomms6360

Winkler, I.G., V. Barbier, B. Nowlan, R.N. Jacobsen, C.E. Forristal, J.T. Patton, J.L. Magnani, and J.P. Lévesque. 2012. Vascular niche E-selectin regulates hematopoietic stem cell dormancy, self renewal and chemoresistance. *Nat. Med.* 18:1651–1657. https://doi.org/10.1038/nm.2969

Wong, S.C., E. Oh, C.H. Ng, and K.P. Lam. 2003. Impaired germinal center formation and recall T-cell-dependent immune responses in mice lacking the costimulatory ligand B7-H2. *Blood.* 102:1381–1388. https://doi.org/10.1182/blood-2002-08-2416

Xu, H., X. Li, D. Liu, J. Li, X. Zhang, X. Chen, S. Hou, L. Peng, C. Xu, W. Liu, et al. 2013. Follicular T-helper cell recruitment governed by bystander B cells and ICOS-driven motility. *Nature.* 496:523–527. https://doi.org/10.1038/nature12058

Yong, P.F., U. Salzer, and B. Grimbacher. 2009. The role of costimulation in antibody deficiencies: ICOS and common variable immunodeficiency. *Immunol. Rev.* 229:101–113. https://doi.org/10.1111/j.1600-065X.2009.00764.x